HAL
archives-ouvertes.fr

Modelling of platelet–fibrin clot formation in flow with a DPD–PDE method

Alen Tosenberger, Fazly Ataullakhanov, Nikolai Bessonov, Mikhail Panteleev, Alexei Tokarev, Vitaly Volpert

▶ **To cite this version:**

Alen Tosenberger, Fazly Ataullakhanov, Nikolai Bessonov, Mikhail Panteleev, Alexei Tokarev, et al.. Modelling of platelet–fibrin clot formation in flow with a DPD–PDE method. Journal of Mathematical Biology, Springer Verlag (Germany), 2015, 10.1007/s00285-015-0891-2 . hal-01237498

HAL Id: hal-01237498
https://hal.archives-ouvertes.fr/hal-01237498

Submitted on 8 Dec 2015

HAL is a multi-disciplinary open access archive for the deposit and dissemination of scientific research documents, whether they are published or not. The documents may come from teaching and research institutions in France or abroad, or from public or private research centers.

L'archive ouverte pluridisciplinaire **HAL**, est destinée au dépôt et à la diffusion de documents scientifiques de niveau recherche, publiés ou non, émanant des établissements d'enseignement et de recherche français ou étrangers, des laboratoires publics ou privés.

Noname manuscript No.
(will be inserted by the editor)

Modelling of platelet-fibrin clot formation in flow with a DPD-PDE method

A. Tosenberger · F. Ataullakhanov · N. Bessonov · M. Panteleev · A. Tokarev · V. Volpert

Received: date / Accepted: date

Abstract The paper is devoted to mathematical modelling of clot growth in blood flow. We investigate the interaction of platelet aggregation with chemical reactions of blood coagulation in plasma. We develop a hybrid DPD-PDE model where Dissipative Particle Dynamics (DPD) is used to model plasma flow and platelets, while the protein regulatory network is described by a system of partial differential equations. We propose a mechanism of clot growth where at the first stage of clot formation platelets form an aggregate due to weak inter-platelet connections and then due to their activation. This enables the formation of the fibrin net in the centre of the platelet aggregate where the flow velocity is significantly reduced. The fibrin net reinforces the clot and allows its further growth. When the clot becomes sufficiently large, it stops growing due to the narrowed vessel and the increase of flow shear rate at the surface of the clot. Its outer part is detached by the flow revealing the inner part covered by fibrin. It does not allow new platelets to attach, and the clot stops growing. Dependence of the final clot size on wall shear rate and on other parameters is studied.

Keywords blood coagulation · clot growth · hybrid models · Dissipative Particle Dynamics

Mathematics Subject Classification (2000) 92C35 · 92C50 · 74F10

A. Tosenberger · V. Volpert
Institut Camille Jordan, UMR 5208 CNRS, University Lyon 1, Lyon, France
E-mail: tosenberger@math.univ-lyon1.fr

F. Ataullakhanov · M. Panteleev · A. Tokarev
National Research Center for Haematology, Ministry of Health and Social Development of Russian Federation, Moscow, Russian Federation

N. Bessonov
Institute of Mechanical Engineering Problems, Saint Petersburg, Russian Federation

1 Introduction

1.1 Biological background

Haemostasis is a physiological process in higher animals by which blood loss is minimized in a case of a vessel injury. As such it is one of the most important survival mechanisms in an individual. The process of haemostasis is based on a complex interaction between four different systems: the vascular system, blood cells, coagulation pathways, and fibrinolysis. In a case of an injury platelets adhere to the injury site and form a primary plug which reduces the blood loss. The plug is reinforced in the process of blood coagulation, in which a network of complex reactions is initiated between proteins in blood. Blood coagulation results in a transformation of plasma into a solid fibrin polymer network which strengthens the platelet plug and completely stops the bleeding. Once the wound is healed, the clot is unnecessary and can obstruct the flow in the vessel. Thus the process of blood coagulation is followed by the process called fibrinolysis during which the clot is decomposed. Haemostasis rests on a sensitive balance between the involved systems and is driven by both prothrombotic and anti-thrombotic factors. A malfunction of any of the systems can cause an imbalance in the haemostatic process. The imbalance can result in a severe blood loss, or it can also lead to the initiation of blood coagulation inside of an uninjured vessel and consequently to the formation of blood clots and the obstruction of the flow. Both cases can have lethal consequences, while the latter case, thrombosis, is the leading immediate cause of mortality and morbidity in the modern society and a major cause of complications in people admitted to hospitals [1].

Due to its importance, haemostasis has been in a focus of research interest since the early beginnings of the medicine. The extensive research in the last century led to precise descriptions of the blood coagulation process in vitro. Two models of the coagulation pathways have emerged - the intrinsic and the extrinsic pathway. Both pathways converge to the so called common pathway, which describes prothrombin to thrombin activation and the process of formation of fibrin polymers. Although the intrinsic and extrinsic pathways are crucial in explaining the observations made using the standard in vitro screening tests, the two pathways do not exist separately in vivo. This has led a to description of the coagulation process in vivo consisting of two phases: the initiation phase, in which a small amount of thrombin is produced due to a presence of tissue factor, and the amplification phase, in which thrombin is produced in a self-accelerated reaction, enabling the formation of fibrin polymers. Although, the key factors in blood coagulation are well investigated and known, due to the immense complexity of the whole haemostatic process, the involved systems and their interactions, the regulation of haemostatic mechanism in vivo still remains poorly understood. One of the most important questions is which mechanisms differentiate haemostasis from thrombosis. The existing anticoagulants cannot tell them apart and target indiscriminately (that is why it is impossible to prevent coronary artery thrombosis simply by putting all high

risk patients on an anticoagulation therapy: the possibility of death caused by external bleeding or cerebral haemorrhaging would become too high). Answering this question would enable a development of drugs which could prevent development of thrombi and, at the same time, would not influence so much the normal process of haemostasis. The answer lies in a better understanding of underlying mechanisms of haemostasis. One of these mechanisms is the process by which the platelet clot and the blood clot stop growing before they obstruct the blood flow through the vessel. While mechanisms of clot growth became well understood during the last decade [2], the process of regulation of clot size remains unclear. Numerous hypotheses have been proposed in the attempt to explain how clot stops growing (e.g. the role of thrombomodulin [3]). One of them is based on the interaction between the platelet and the fibrin clot. The hypothesis states that the formation of a fibrin cap on the surface of the clot is responsible for preventing a further platelet accumulation [4]. However, the formation of fibrin on the surface of a clot is unlikely because of high shear rates that remove active coagulation factors [5]. So far none of these hypothesis has given a satisfactory answer, nor any of them has been experimentally confirmed. Hence, in the focus of this work is to give a possible explanation of the mechanisms of the clot growth arrest by development of a hybrid mathematical model describing the problem on multiple scales.

1.2 Methods of modelling

The previous works on modelling of blood coagulation in flow used different approaches. The models can be divided in three main subgroups: continuous, discrete and hybrid models. The first group, continuous models, is based on the mathematical knowledge of partial differential equations and numerical schemes to solve them [6,7,8,9,10,11]. In such models PDEs are used either to describe the blood as a homogeneous fluid with non-Newtonian properties, or to describe blood plasma as a Newtonian fluid (Navier-Stokes equations) with blood cells described in terms of concentrations. Although such models can accurately describe the flow properties together with the diffusion and reactions of protein concentrations in blood flow, they fail to account for individual cell behaviour and cell interactions. Discrete models, on the other hand, make modelling of individual cells feasible, and by use of simulation methods like Smoothed-Particle Hydrodynamics (SPH), Lattice Gas Automata (LGA), Lattice Boltzmann (LB) and Dissipative Particle Dynamics (DPD) the hydrodynamic behaviour can be correctly reproduced. Where discrete methods come short is in the description of protein concentrations, and their diffusion and reactions in flow. The third group, hybrid models, tries to avoid pitfalls of both continuous and discrete approaches by combining them together. Such methods are suitable for modelling of blood flow, individual blood cells, protein concentrations and reactions. Therefore, in the last decade several different hybrid approaches have been developed to study blood coagulation in flow. A number of them uses the continuous concept to model blood flow and

propagation of blood factors in it, while the discrete concept is used to model blood cells and their interactions. In [12,14,15,16,17,18,19] blood flow is described by Navier-Stokes equations. The motion of blood cells in blood flow then follows from the calculated velocity field. As the flow simulation domain changes because of clot growth, the Immersed Boundary (IB) method is often used. The protein cascade is described with a system of differential equations, each describing a concentration of a single blood factor. Blood cells and their interactions are modelled with a discrete method like Cellular Potts Method (CPM) or Subcellular Element Method (SCE).

A DPD-PDE hybrid method was considered in [22]. The DPD method was used to model blood plasma flow and platelets, while concentrations of proteins were described by convection-diffusion equations in order to model agonists which induce platelet activation. It is supposed that these agonists are produced by platelets in flow or in the platelet aggregate at the injury site. The agonists then diffuse in flow and activate platelets if their concentration around those platelets reaches a certain threshold. Once activated, the platelets can aggregate to each other or adhere to the vessel wall at the injury site. The main goal in [22] was to develop a model of platelet aggregation based on the assumption that platelet activation precedes platelet aggregation. However, this model was not used to study the mechanisms of clot growth and growth arrest.

In our work we develop a new DPD-PDE hybrid model of clot growth in blood flow. DPD is a well-established simulation method for modelling of hydrodynamics. Whereas there are more computationally efficient methods than DPD for simulating simple fluids, the advantage of DPD is that it is also suitable for modelling of complex fluids, such as blood [23,37,44,45]. In our model we use DPD to simulate blood plasma flow and platelets. The DPD method is coupled with a system of partial differential equations which describe concentrations of blood factors (thrombin, fibrinogen, and fibrin polymer), their diffusion and reactions in flow. Blood factors are assumed either to be constantly present in the flow (fibrinogen produced in liver circulates in blood) or to be produced or activated at the injury site (thrombin activation at the injury site initiated by tissue factor).

The model developed in this paper is based on the approach described in the previous works of the authors: purely discrete models of platelet aggregation in a blood plasma flow [20] and a simplified hybrid model of clot formation in flow where fibrin concentration is modelled with a single advection-reaction-diffusion equation [21]. In [21] we have introduced a DPD-PDE method on model examples and showed that it can be used in modelling of blood coagulation and clot growth. Here we suggest a more complete and biologically more realistic model of blood coagulation then it was done in [21] and we use it to study the mechanism of clot growth in flow. The main difference with [22] is that we consider different blood factors in order to study blood coagulation and we do not assume that platelet activation precedes their aggregation. This is an important assumption which will be discussed below.

1.3 Main assumptions and results of this work

Biological assumptions. An important aspect of the blood coagulation modelling concerns the biological assumptions of the model. In most of previous works it was assumed that platelet activation precedes platelet aggregation [2,23,12,14,15,16,17,22,24,25]. Platelet activation can occur because of platelet's interaction with other activated platelets [23,12] or with biochemical substances in blood plasma [14,15,16,17,22,25]. However, recent results show that activation may not precede aggregation [24,26,27,28,29,30,31]. This new understanding of platelet aggregation is based on several observations. Firstly, platelet activation is not instantaneous (by some estimates it can take from several seconds up to one minute [32]), while platelet aggregation begins right after the injury. Secondly, if activation would precede aggregation, then platelets would need to be activated at a certain distance before arriving to the injury site. As platelets are activated by blood factors, the previous assumption would imply that concentrations of blood proteins diffuse from the injury site in the direction against the flow. If the flow speed is sufficiently high, this assumption becomes unrealistic. Thus we come to the conclusion that platelets can aggregate in the clot without activation. This is confirmed by biological observations [24,26,27,28,29,30,31]. Therefore, in the model described in this paper it is assumed that platelet aggregation precedes platelet activation. Another biological assumption on which the model is based on is that the fibrin polymer net reinforces the structure of the platelet clot, but at the same time makes platelets which are covered by it resistant to further platelet adhesion. Although platelets from the flow can bind directly to fibrin [27,28,30], instead to platelets covered by it, such bonding is rather weak and does not leat to platellet activation, thus it cannot sustain high shear rates. The non-adhesive effect of fibrin polymers has been observed experimentally [4].

Main results. The main goal of this work is to suggest a possible explanation of the mechanisms of clot growth and growth arrest. Our results allow us to propose the following mechanisms. At first, a weak platelet aggregate forms at the injury site. Platelets are not yet activated but they can still aggregate due to GPIb receptors. After a short time delay, their activation begins and reinforces their connections. Flow velocity decreases inside the platelet aggregate. Because of this, thrombin produced at the injury site accumulates inside the platelet aggregate and initiates the formation of a fibrin net. The fibrin net reinforces the platelet aggregate even more, making the clot more stable and allowing its further growth. The clot growth leads to a narrowing of the vessel and the increase of the flow shear rate at the surface of the clot. It results in eliminating of the outer parts of the platelet aggregate which are not covered by fibrin polymer. The remaining clot is covered by fibrin and it cannot grow further. There are two possible situations. In the first case the remaining clot is completely covered by the fibrin net, which makes the platelets that are captured within, non-adhesive. Thus they cannot aggregate with platelets from

the flow. In the second case the remaining clot is almost completely covered by the fibrin net. Due to high shear rate at the clot surface, and the fact that newly aggregated platelets need some time to activate or become covered by the fibrin net, the newly aggregated platelets are not able to establish stronger bonds and are thus taken by the flow.

It is important to emphasize that there exist biochemical mechanisms which stop coagulation cascade in a quiescent plasma without platelets. However, there are additional mechanisms which stop clot growth in flow. Indeed the clot size depends on the acute rate of clot growth and on the duration of the acute phase [59], thus it implicitly depends on the vessel diameter, the flow velocity and other parameters. This cannot be explained only by the biochemical reactions in plasma, such as protein C pathway [57,58]. We discuss the mechanisms specific for clot growth and arrest in flow. They are based on the interaction between the platelet aggregation and the formation of the fibrin net. We will study how the final clot size depends on various parameters. We will see in particular how wall shear rate and vessel diameter can play an important role in the clot formation.

2 DPD-PDE hybrid model

In this work we use the DPD-PDE approach to describe clot growth in blood flow. Dissipative particle dynamics (DPD) is used to model blood plasma and platelets. Platelets are considered as small soft spheres which can interact with fluid particles and with each other. They can aggregate in the flow or in the clot and can also detach if the force pulling them away is greater than a certain limit. Partial differential equations are used in order to describe concentrations of biochemical substances in plasma, such as fibrin. Interaction of fibrin with platelets plays an important role in biology of clot growth and in the model studied below.

2.1 Flow model

We use the Dissipative Particle Dynamics (DPD) method in the form described in literature [33,34,35]. It is a mesoscale method, meaning that each DPD particle describes some small volume of a simulated medium rather than an individual molecule. The method is governed by three equations describing the conservative, dissipative and random force acting between each two particles:

$$\mathbf{F}_{ij}^C = F_{ij}^C(r_{ij})\hat{\mathbf{r}}_{ij}, \tag{1}$$

$$\mathbf{F}_{ij}^D = -\gamma\omega^D(r_{ij})(\mathbf{v}_{ij}\cdot\hat{\mathbf{r}}_{ij})\hat{\mathbf{r}}_{ij}, \tag{2}$$

$$\mathbf{F}_{ij}^R = \sigma\omega^R(r_{ij})\frac{\xi_{ij}}{\sqrt{dt}}\hat{\mathbf{r}}_{ij}, \tag{3}$$

where $\mathbf{r}_i$ is the vector of position of the particle i, $\mathbf{r}_{ij} = \mathbf{r}_i - \mathbf{r}_j$, $r_{ij} = |\mathbf{r}_{ij}|$, $\hat{\mathbf{r}}_{ij} = \mathbf{r}_{ij}/r_{ij}$, and $\mathbf{v}_{ij} = \mathbf{v}_i - \mathbf{v}_j$ is the difference between velocities of two particles, γ and σ are coefficients which determine the strength of the dissipative and the random force respectively, while ω^D and ω^R are weight functions; ξ_{ij} is a normally distributed random variable with zero mean, unit variance, and $\xi_{ij} = \xi_{ji}$. The conservative force is given by the equality

$$F_{ij}^C(r_{ij}) = \begin{cases} a_{ij}\left(1 - r_{ij}/r_c\right) & \text{for } r_{ij} \le r_c, \\ 0 & \text{for } r_{ij} > r_c, \end{cases} \tag{4}$$

where a_{ij} is the conservative force coefficient between particles i and j, and r_c is the cut-off radius.

The random and dissipative forces form a thermostat. If the following two relations are satisfied, the system will preserve its energy and maintain the equilibrium temperature:

$$\omega^D(r_{ij}) = \left[\omega^R(r_{ij})\right]^2 q^2 = 2\gamma k_B T, \tag{5}$$

where k_B is the Boltzmann constant and T is the temperature. The weight functions are determined by:

$$\omega^R(r_{ij}) = \begin{cases} \left(1 - r_{ij}/r_c\right)^k & \text{for } r_{ij} \le r_c, \\ 0 & \text{for } r_{ij} > r_c, \end{cases} \tag{6}$$

where $k = 1$ for the original DPD method, but it can be also varied in order to change the dynamic viscosity of the simulated fluid [33]. The motion of particles is determined by Newton's second law of motion:

$$d\mathbf{r}_i = \mathbf{v}_i dt, \quad d\mathbf{v}_i = \frac{dt}{m_i} \sum_{j \ne i} \left(\mathbf{F}_{ij}^C + \mathbf{F}_{ij}^D + \mathbf{F}_{ij}^R\right), \tag{7}$$

where m_i is the mass of the particle i.

The simplest way to integrate the equations of motion (7) is by use of Euler method:

$$\mathbf{v}_i^{n+1} = \mathbf{v}_i^n + \frac{1}{m_i}\mathbf{F}_i\left(\mathbf{r}_i^n, \mathbf{v}_i^n\right) dt, \tag{8}$$

$$\mathbf{r}_i^{n+1} = \mathbf{r}_i^n + \mathbf{v}_i^{n+1} dt, \tag{9}$$

where indices n and $n+1$ denote time steps, and

$$\mathbf{F}_i = \sum_{j \ne i} \left(\mathbf{F}_{ij}^C + \mathbf{F}_{ij}^D + \mathbf{F}_{ij}^R\right). \tag{10}$$

Instead of the conventional Euler method, a more refined method, called modified velocity-Verlet method, can be used [34,36]. First described by Groot and Warren in 1997, it is more accurate and it allows a certain increase in time

step dt, thus reducing the computational cost of a simulation. The discretization of the equations (7) by modified velocity-Verlet scheme is given by:

$$\mathbf{r}_i^{n+1} = \mathbf{r}_i^n + \mathbf{v}_i^n dt + \frac{1}{2}\mathbf{a}_i^n dt^2, \tag{11}$$

$$\mathbf{v}_i^{n+\frac{1}{2}} = \mathbf{v}_i^n + \frac{1}{2}\mathbf{a}_i^n dt, \tag{12}$$

$$\mathbf{a}_i^{n+1} = \frac{1}{m_i}\mathbf{F}_i\left(\mathbf{r}_i^{n+1}, \mathbf{v}_i^{n+\frac{1}{2}}\right), \tag{13}$$

$$\mathbf{v}_i^{n+1} = \mathbf{v}_i^{n+\frac{1}{2}} + \frac{1}{2}\mathbf{a}_i^{n+1} dt, \tag{14}$$

where a_i^n denotes the acceleration of the particle i at the n^{th} time step. Both methods give close results.

In scope of this work a new method was also used. The method can be considered as a semi-implicit in the context of the dissipative force, as it takes implicitly a part of the velocity term in the calculation of the dissipative force. Let us write a sum of DPD forces on some particle i:

$$\mathbf{F}_i = \sum_j \left(\mathbf{F}_{ij}^C(\mathbf{r}_i, \mathbf{r}_j) + \mathbf{F}_{ij}^D(\mathbf{r}_i, \mathbf{r}_j, \mathbf{v}_i, \mathbf{v}_j) + \mathbf{F}_{ij}^R(\mathbf{r}_i, \mathbf{r}_j)\right). \tag{15}$$

where the conservative and the random force depend only of positions of particles i and j, while the dissipative force depends additionally of particles' velocities. Let us take the velocity of the particle i in the implicit form and the remaining variables in the explicit form:

$$\mathbf{F}_i = \sum_j \left(\mathbf{F}_{ij}^C(\mathbf{r}_i^n, \mathbf{r}_j^n) + \mathbf{F}_{ij}^D(\mathbf{r}_i^n, \mathbf{r}_j^n, \mathbf{v}_i^{n+1}, \mathbf{v}_j^n) + \mathbf{F}_{ij}^R(\mathbf{r}_i^n, \mathbf{r}_j^n)\right). \tag{16}$$

By including it in the first step of Euler integration method (equation (8)) the following equation is obtained :

$$\mathbf{v}_i^{n+1} = \mathbf{v}_i^n + \frac{dt}{m_i}\sum_j \left(\mathbf{F}_{ij}^C(\mathbf{r}_i^n, \mathbf{r}_j^n) + \mathbf{F}_{ij}^D(\mathbf{r}_i^n, \mathbf{r}_j^n, \mathbf{v}_i^{n+1}, \mathbf{v}_j^n) + \mathbf{F}_{ij}^R(\mathbf{r}_i^n, \mathbf{r}_j^n)\right). \tag{17}$$

After expanding the dissipative force to its full form given by the equation (2) and placing all of the expressions multiplying $\mathbf{v}_i^{n+1}$ on the left side one obtains:

$$\begin{aligned} &\mathbf{v}_i^{n+1} + \frac{dt}{m}\sum_j \gamma\omega^D(r_{ij}^n)(\mathbf{v}_i^{n+1}\cdot\hat{\mathbf{r}}_{ij}^n)\hat{\mathbf{r}}_{ij}^n = \\ &= \mathbf{v}_i^n + \frac{dt}{m_i}\sum_j \left(\mathbf{F}_{ij}^C(\mathbf{r}_i^n, \mathbf{r}_j^n) + \gamma\omega^D(r_{ij}^n)(\mathbf{v}_j^n\cdot\hat{\mathbf{r}}_{ij}^n)\hat{\mathbf{r}}_{ij}^n + \mathbf{F}_{ij}^R(\mathbf{r}_i^n, \mathbf{r}_j^n)\right), \end{aligned} \tag{18}$$

where $\mathbf{r}_{ij} = \mathbf{r}_i - \mathbf{r}_j$, $r_{ij} = |\mathbf{r}_{ij}|$ and $\hat{\mathbf{r}}_{ij} = \mathbf{r}_{ij}/r_{ij}$. Now the left side of the equation (18) can be written as:

$$\mathbf{v}_i^{n+1}\left(I+\frac{dt}{m}\sum_j \gamma\omega^D(r_{ij}^n)(\hat{\mathbf{r}}_{ij}^n\otimes\hat{\mathbf{r}}_{ij}^n)\right)= \tag{19}$$
$$=\mathbf{v}_i^n+\frac{dt}{m_i}\sum_j\left(\mathbf{F}_{ij}^C(\mathbf{r}_i^n,\mathbf{r}_j^n)+\gamma\omega^D(r_{ij}^n)(\mathbf{v}_j^n\cdot\hat{\mathbf{r}}_{ij}^n)\hat{\mathbf{r}}_{ij}^n+\mathbf{F}_{ij}^R(\mathbf{r}_i^n,\mathbf{r}_j^n)\right).$$

Set

$$A=I+\frac{dt}{m}\sum_j\gamma\omega^D(r_{ij}^n)(\hat{\mathbf{r}}_{ij}^n\otimes\hat{\mathbf{r}}_{ij}^n). \tag{20}$$

Lemma 1 *If $\mathbf{v}_i\in\mathbb{R}^n$ for $i=1,\dots,k$ and $\alpha_i\in\mathbb{R}$, $i=1,\dots,k$, such that $\alpha_i\geq 0$, $\forall i$, then the matrix $A=I+\sum_{j=1}^{k}\alpha_j\left(\mathbf{v}_j\otimes\mathbf{v}_j\right)$ is invertible.*

Proof Let us first define matrices A_i as

$$A_i=\alpha_i\left(\mathbf{v}_i\otimes\mathbf{v}_i\right), \qquad \text{for } i=1,\dots k. \tag{21}$$

Let us first note that matrices A_i, $i=1,\dots,k$, are symmetric and positive semi-definite as for any vector $\mathbf{x}\in\mathbb{R}^n$ we have:

$$\mathbf{x}^\tau A_i\mathbf{x}=\alpha_i\begin{pmatrix}x_1 & \dots & x_n\end{pmatrix}\begin{pmatrix}v_1^2 & \dots & v_1v_n\\ \vdots & \ddots & \vdots\\ v_nv_1 & \dots & v_n^2\end{pmatrix}\begin{pmatrix}x_1\\ \vdots\\ x_n\end{pmatrix} \tag{22}$$

$$=\alpha_i\begin{pmatrix}v_1\sum_{i=1}^n x_iv_i & \dots & v_n\sum_{i=1}^n x_iv_i\end{pmatrix}\begin{pmatrix}x_1\\ \vdots\\ x_n\end{pmatrix} \tag{23}$$

$$=\alpha_i\sum_{j=1}^n\left(x_jv_j\sum_{i=1}^n x_iv_i\right)=\alpha_i\left(x_1v_1+\dots x_nv_n\right)^2\geq 0. \tag{24}$$

As the identity matrix is positive definite and as the sum $A+B$ of a positive definite matrix A and a positive semi-definite matrix B is positive definite:

$$\begin{aligned}&x^\tau Ax>0, \qquad \forall x\in\mathbb{R}^n, x\neq 0,\\ &x^\tau Bx\geq 0, \qquad \forall x\in\mathbb{R}^n,\\ &x^\tau(A+B)x=(x^\tau A+x^\tau B)x=x^\tau Ax+x^\tau Bx>0, \forall x\in\mathbb{R}^n, x\neq 0,\end{aligned} \tag{25}$$

it follows that $I+\sum_{i=1}^n A_i$ is a positive definite matrix, and as such is invertible.

From Lemma 1 it follows that the matrix A is invertible, so from the equation (19) we can write:

$$\mathbf{v}_i^{n+1} = \Bigg[\mathbf{v}_i^n + \frac{dt}{m_i}\sum_j \Bigg(\mathbf{F}_{ij}^C(\mathbf{r}_i^n, \mathbf{r}_j^n) + \\ + \gamma\omega^D(r_{ij}^n)(\mathbf{v}_j^n \cdot \hat{\mathbf{r}}_{ij}^n)\hat{\mathbf{r}}_{ij}^n + \mathbf{F}_{ij}^R(\mathbf{r}_i^n, \mathbf{r}_j^n)\Bigg)\Bigg] A^{-1}. \tag{26}$$

Once the new velocity of particle i is obtained, its new position can be calculated by the second step of Euler integration method (the equation (9)).

On the one hand the previously described method is not symmetrical as one part of the velocity difference $\mathbf{v}_i - \mathbf{v}_j$ is taken implicitly and the other part explicitly. As a result the particle system does not preserve its total momentum. On the other hand, for a small time step the error does not significantly influence the behaviour of the whole system, and it allows an increase of time step for the DPD method for several orders of magnitude. Because of the loss of symmetry, the method should be used cautiously and results should be verified by comparison to a more precise integration scheme.

The behaviour of DPD method, as well as its suitability for the problem of fluid simulation is well described in literature [33,34,35,37,38]. In [33,37] DPD simulation results are compared with the results obtained by using continuous methods (Navier-Stokes and Stokes equations) for Couette, Poiseuille, square-cavity and triangular-cavity flow.

2.2 Coagulation pathway model

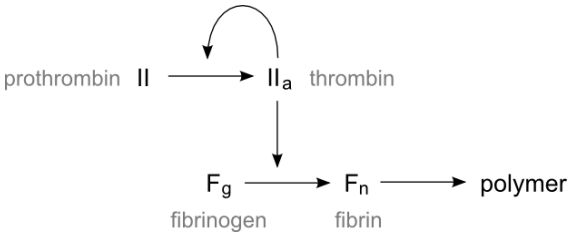

Fig. 1 Blood coagulation pathway, as described in the model. The model takes into account the local production of thrombin due to presence of tissue factor, the self-accelerated thrombin production, and the fibrin polymer production from fibrinogen in the presence of thrombin.

At the next stage of modelling a simplified phenomenological model, shown in Figure 1, was used to describe the protein regulatory network of blood coagulation. The model consists of the self-accelerated production of thrombin from prothrombin, and the fibrin cascade which is influenced by the thrombin

concentration. Instead of a simplest reaction-diffusion-advection equation from the model described in [21], a system of partial differential equations is developed in order to account for the main characteristics of the blood coagulation pathway.

Thrombin reaction. We use the following equation for thrombin concentration T_h:

$$\frac{\partial T_h}{\partial t} = k_1(T_h)(C_0 - T_h) - s_1 T_h, \tag{27}$$

where the first term in the right-hand side describes self-accelerating production of thrombin from prothombin and the second right hand term describes thrombin degradation. C_0 is the initial concentration of prothrombin, $k_1(T_h)$ is a reaction rate function depending on concentration of thrombin T_h (it will be specified bellow), and s_1 is the degradation constant. In order to study blood coagulation in flow (in vivo), diffusion and advection terms are added to the equation (27):

$$\frac{\partial T_h}{\partial t} + \nabla \cdot (\mathbf{v} \cdot T_h) = D_{T_h} \Delta T_h + k_1(T_h)(C_0 - T_h) - s_1 T_h, \tag{28}$$

where D_{T_h} is the thrombin diffusion coefficient, $\mathbf{v}$ is the velocity field. As blood plasma is considered to be incompressible, i.e. with zero divergence, the advection term can be simplified, thus obtaining the following equation for thrombin concentration:

$$\frac{\partial T_h}{\partial t} + \mathbf{v} \cdot \nabla T_h = D_{T_h} \Delta T_h + k_1(T_h)(C_0 - T_h) - s_1 T_h, \tag{29}$$

Fibrin reactions. Consider, next, the reactions

$$F_g \rightarrow F_n \rightarrow F_p, \tag{30}$$

where F_p is fibrin polymer. Unlike thrombin which is produced locally at the injury site and inside the the clot, fibrinogen is synthesized in the liver and constantly circulates in the blood stream. The availability of thrombin, as an enzyme, is necessary to produce fibrin from fibrinogen. Therefore, it is important to take into account the flow influence on both concentrations - thrombin and fibrinogen. We omit fibrin in the reaction scheme (30) and consider instead a simplified reaction $F_g \rightarrow F_p$. Then, the reaction can be represented by the following model:

$$\frac{\partial F_g}{\partial t} + \mathbf{v} \cdot \nabla F_g = D_{F_g} \Delta F_g - k_3(T_h) F_g, \tag{31}$$

$$\frac{\partial F_p}{\partial t} = k_3(T_h) F_g, \tag{32}$$

where D_{F_g} is the fibrinogen diffusion coefficient, and $k_3(T_h)$ is the reaction constant which depends on the concentration of thrombin. The equation (31)

describes fibrinogen diffusion in flow, and the equation (32) describes the concentration of fibrin polymers which form an insoluble network and thus do not diffuse or flow.

Coagulation pathway model. By combining the equation(29) for thrombin concentration, and equations (31) and (32) for fibrinogen and fibrin polymer concentrations respectively, one obtains the following model:

$$\begin{aligned} \frac{\partial T_h}{\partial t} + \mathbf{v} \cdot \nabla T_h &= D_{T_h} \Delta T_h + k_1(T_h)(C_0 - T_h) - s_1 T_h, \\ \frac{\partial F_g}{\partial t} + \mathbf{v} \cdot \nabla F_g &= D_{F_g} \Delta F_g - k_3(T_h) F_g, \\ \frac{\partial F_p}{\partial t} &= k_3(T_h) F_g. \end{aligned} \tag{33}$$

In order to model self-amplifying thrombin reaction, the reaction function $k_1(T_h)$ is defined as follows:

$$k_1(T_h) = k_1^0 \frac{T_h^2}{T_0 + T_h}, \tag{34}$$

where k_1^0 and T_0 are constants. The function (34) is based on the Michaelis–Menten equation, but at low thrombin concentration it has a lower gradient than the Michaelis-Menten equation. While the thrombin equation from equations (33) with a Michaelis-Menten term would be a monostable problem, with the term from equation (34) is becomes a bistable problem. Thus, if the thrombin concentration is too low, with time it will converge to zero.

The fibrin reaction rate coefficient $k_3(T_h)$ is for simplicity taken to be linear:

$$k_3(T_h) = k_3^0 T_h. \tag{35}$$

In both the initiation and the amplification phase of blood coagulation in vivo a complex pathway precedes the prothrombin-thrombin reaction. In the initiation phase this part of the pathway is initiated by tissue factor which is normally present in sub-endothelial fibroblasts, injured vascular endothelium and activated monocytes. Once vessel wall is injured tissue factor enters the blood flow nearby and starts the coagulation cascade. In the amplification phase thrombin concentration acts as enzyme in activation of cofactors which accelerate prothrombin-thrombin reaction, thus causing explosive increase in thrombin concentration. The self-amplification effect of thrombin reaction is modelled by equation (34). In order to model the localized generation of thrombin near the vessel injury site, in the model the initial value of the thrombin concentration is set to zero in the whole domain except on the part of boundary where injury site is located and where the concentration is set to a non-zero value (equation (37)). This corresponds to the initial concentration of thrombin, produced due to the presence of tissue factor at the

injury site. As thrombin concentration equation (equation (29)) is bistable, the initial non-zero concentration at the boundary has to be high enough to start thrombin accumulation, otherwise concentration will quickly decrease to zero. At all domain boundaries Neumann boundary conditions are used:

$$\left.\frac{\partial T_h}{\partial x}(x,y,t)\right|_{x=0,L} = \left.\frac{\partial T_h}{\partial y}(x,y,t)\right|_{y=0,D} = 0 \tag{36}$$

$$\left.T_h(x,y,t)\right|_{t=0} = \begin{cases} 1, & \text{if } x \in [w_B, w_E] \text{ and } y = 0, \\ 0, & \text{if } x \notin [w_B, w_E] \text{ or } y \neq 0, \end{cases} \tag{37}$$

where $[0, L] \times [0, D]$ is the simulation domain, i.e. a part of blood vessel of the length L and diameter D, and where $[w_B, w_E] \times \{0\}$ is the part of domain representing the vessel injury site.

The primary function of thrombin is conversion of fibrinogen to fibrin. Fibrinogen, being synthesised in liver by hepatocytes, is constantly present in a healthy bloodstream. Therefore, in the model, the initial concentration of fibrinogen is set to some value F_g^0 in the whole domain and Dirichlet boundary conditions are used at the inflow boundary, while the remaining boundaries are described with zero Neumann boundary conditions:

$$\left.\frac{\partial F_g}{\partial x}(x,y,t)\right|_{x=L} = \left.\frac{\partial F_g}{\partial y}(x,y,t)\right|_{y=0,D} = 0, \tag{38}$$

$$\left.F_g(x,y,t)\right|_{x=0} = F_g^0, \tag{39}$$

$$\left.F_g(x,y,t)\right|_{t=0} = F_g^0. \tag{40}$$

2.3 Platelet aggregation

Platelets are modelled as soft spherical particles similar to the particles of fluid in DPD. The radius of all particles (fluid and platelets) and their mass are chosen to correspond to the radius and the mass of platelets. In our simulation the physical radius is set to 1μm and the mass is chosen in such a way that particle density corresponds to the physiological density of the blood plasma ($\approx 10^3 \text{kg/m}^3$). Interactions between all particles are then governed by DPD as described in the previous section with an additional adhesion force acting between platelets. By the virtue of the mechanical properties of the clot [39, 40], the adhesion force is modelled as a pairwise force between two platelets expressed in the form of Hooke's law:

$$\mathbf{F}_{ij}^{A} = f^{A}(t_{ij}) \left(1 - \frac{r_{ij}}{d_C}\right) \hat{\mathbf{r}}_{ij}, \tag{41}$$

where f^A is the force strength coefficient and d_C is the force relaxation distance which is equal to two times the physical radius of the platelets. As platelet binding occurs due to their surface adhesion receptors, two platelets in flow connect when they come in physical contact, i.e. $r_{ij} \leq d_C$ (connection criterium). Platelets remain connected for as long as their distance does not exceed some critical value d_D (disconnection criterium) which is greater than d_C. We set d_D equal to 1.3 times of the platelet diameter. The force strength coefficient f^A in equation (41) is modelled in the following way to describe three strengths of different inter-platelet bonds:

$$f^{A}(t_{ij}) = \begin{cases} f_1^A & \text{if } F_p(i) \text{ or } F_p(j) < c_{F_p}, \quad \text{and} \quad t_{ij} < t_c, \\ f_2^A & \text{if } F_p(i) \text{ or } F_p(j) < c_{F_p}, \quad \text{and} \quad t_{ij} \geq t_c, \\ f_3^A & \text{if } F_p(i) \text{ and } F_p(j) \geq c_{F_p}, \end{cases} \tag{42}$$

where $f_1^A < f_2^A < f_3^A$ are the three strengths of inter-platelet connections, representing respectively a weak bond due to GPIb receptors, a medium bond due to platelet activation and a strong bond due to reinforcement by fibrin polymer net. t_c is the time needed for platelet activation measured from the moment of the connection establishing. As the platelet activation process is not at the focus of this study, activation period serves as a basic approximation of the platelet activation process due to the contact and proximity of other activated platelets (ex. activation due to secretion of ADP). $F_p(i)$ and $F_p(j)$ are levels of fibrin polymer F_p at the positions of particles i and j respectively. c_{F_p} is the critical level of fibrin polymer. A platelet is considered to be a part of the clot core if it is in the clot and the fibrin concentration has been larger than c_{F_p} at the position of that platelet. Therefore, the clot core is a part of clot covered by a concentration of F_p larger than c_{F_p}. As the platelets that are coated in fibrin are adhesion resistant [4], the same condition is applied in the model in a way that the platelets of the clot core cannot establish new connections with the platelets in the flow. In the case of physical contact between two platelets that are not connected, one of which is non-adhesive, an additional repulsing force has to be introduced between them in order to prevent them from occupying the same space.

3 Results

A typical clot structure is shown in Figure 2. There are three types of platelet connections, weak (light red lines between their centres), medium (dark red lines) and strong (black lines). Medium connections appear if platelets are weakly connected during the time period t_c. Hence we model platelet activation and emergence of medium connections as a time delay. Platelets covered by

fibrin are shown with dark green colour, platelets not covered by fibrin with light green.

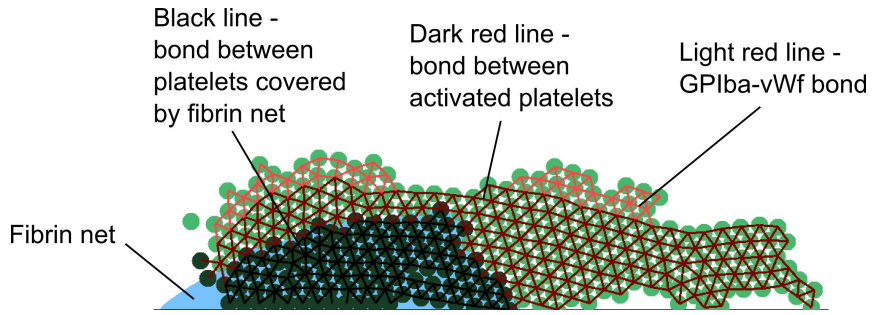

Fig. 2 A scheme of clot structure (snapshot from simulation presented in Figure 3). Connections between platelets are shown as red intervals between their centres. Light red lines correspond to weak GPIb connections, dark red to medium connections between activated platelets, and black to strong connections between platelets covered by a fibrin net. Dark green platelets are covered by fibrin net, which is marked by blue color.

In the basic simulation the values of parameters were chosen in such a way that they correspond to the vessel of $50\mu m$ in diameter and 200 to 300 μm long. The density and the viscosity of the simulated medium were chosen to correspond to the density and the viscosity of blood plasma [41] ($\approx 1.24m$Pa·s). The average velocity of the flow is chosen to be 18.75 mm/s, which in a vessel of $50\mu m$ in diameter produces a wall shear rate of 1500 s^{-1}. To initiate clotting, at the beginning of the simulation, several stationary platelets are positioned at the injury site next to the lower vessel wall. Table 1 (see Appendix) lists all the values of parameters chosen for the basic simulation. The values are considered in the following system of physical units: 10^{-6}m (=1μm), $10^{-14}kg$ (=10pg), and 10^{-2}s (=10ms). As the model of coagulation pathways is phenomenological, the concentration scale is left in the non-dimensional form. In the table, the values of all parameters are expressed in both forms - as used in the simulations and interpreted in the standard SI units system.

Depending on the values of parameters of concentration equations, for any given flow properties there exist two limiting scenarios of the propagation of the thrombin concentration. In the first scenario the thrombin concentration decreases due to diffusion, degradation and outflow until it rests at zero value in the whole domain. As the ending result the fibrin net does not form. In the second scenario thrombin generation is too high, resulting in thrombin propagation outside of the platelet aggregate and finally in a rapid formation of fibrin net outside of the platelet clot. Values of some parameters, like diffusion coefficients, were taken from the continuous model of blood coagulation by Krasotkina et al. [42], where they were related to experimental data. Values of the remaining parameters were varied in order to account for all possible model behaviours which lie between the two limiting scenarios.

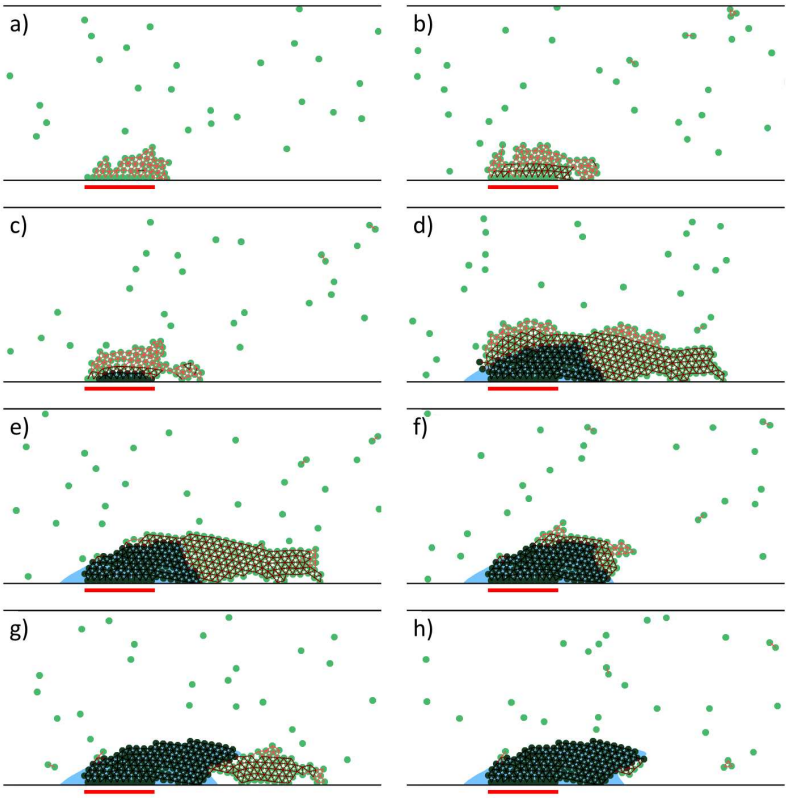

Fig. 3 Example of clot growth with the indicated concentration of fibrin polymer. Simulation snapshots show the following stages of the clot growth: a) a clot begins to grow by formation of a platelet aggregate, b) some of the aggregated platelets activate allowing the clot to grow larger, c) fibrin begins to cover the growing clot allowing the clot to grow further, d) the clot reaches its critical size, e,f,g) parts of clot not covered by the fibrin net rupture and are taken by the flow, h) the last rupture leaves only the adhesion resistant clot core, which prevents the clot from growing further. The snapshots are obtained for values of parameters as presented in Table 1, except for the following values: $f_1^A = 0.5$ nN, $f_2^A = 0.8$ nN, $t_c = 0.4$ s.

3.1 Model behaviour

Several stages of clot growth and the evolution of thrombin, fibrinogen and fibrin polymer concentration profiles protected by the clot are shown in Figure 3 and Figure 4. In the beginning of clot growth, platelets aggregate at the injury site due to weak connections. The injury site is modelled as several platelets attached to the vessel wall. They initiate platelet clot growth. The platelets gradually become activated enabling the aggregate to grow further. The flow velocity inside the newly formed platelet aggregate decreases, and becomes insignificant compared to the bulk flow velocity. It makes possible for the coagulation reactions to commence, hence the thrombin concentration

gradually increases due to the self-accelerated reaction (equations (33) and (34)). With thrombin being present, the production of fibrin polymer from fibrinogen (and implicitly fibrin) begins, and fibrin polymer accumulates inside the platelet clot. When F_p concentration exceeds the critical level c_{F_p}, it is considered that the fibrin net, and with it the clot core have been formed at that place. By this mechanism, the fibrin net forms inside the platelet clot and reinforces the inter-platelet bonds, creating the clot core and allowing a further growth of the clot. The growing clot narrows the blood vessel. As a result, the shear stress on on the top of the clot increases. The platelet aggregates, which are on the outer part of the clot and are not yet covered by the fibrin net, come under much larger stress and are taken by the flow one by one. This leaves only the part of the clot which is either completely or mostly covered by fibrin net. The remaining clot is stable due to being reinforced by the fibrin net, but at the same time it cannot grow any further, thus the clot growth is stopped. In the case when the remaining clot is completely covered by the fibrin net, platelets in the clot cannot attach new platelets from the flow due to the non-adhesive effect of fibrin-polymers [4]. In the case when the remaining clot is almost completely covered by the fibrin net, the new platelets from flow can aggregate at the surface of the clot which is not yet covered by the fibrin net. However, the platelet activation takes some time and the shear stress at the clot surface is high. Because of that the newly aggregated platelets are being taken by the flow before they can activate and form more stable bonds.

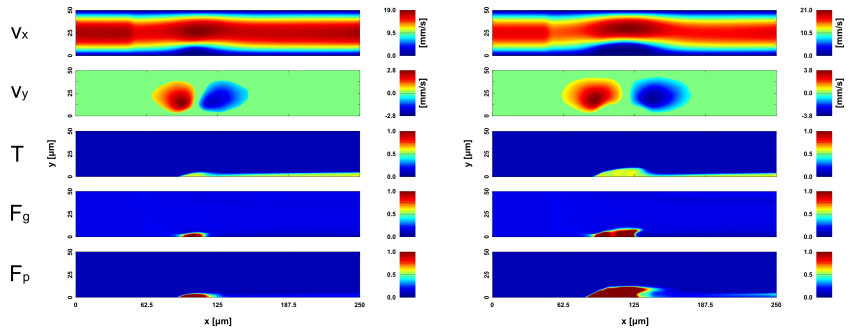

Fig. 4 Velocity and concentration profiles for two stages of clot growth: clot in growth (left) and after the growth arrest (right). From top to bottom: the component of velocity tangential to the vessel wall, the component of velocity orthogonal to the vessel wall, thrombin concentration, fibrinogen concentration, fibrin polymer concentration.

The platelet concentration in simulations is set to $3.672 \cdot 10^{12}$ L^{-1} which is 9.17 to 24.48 times higher than the experimentally observed concentration [43]. This is done to obtain a full clot evolution in less simulation time. However, in the model platelets are uniformly distributed in the vessel cross-section, while in vivo they are concentrated closer to the vessel wall because they are pushed there by erythrocytes [44,45]. Hence, the acceleration of clot growth in simu-

lations is much lower than the nominal increase in the platelet concentration. All this does not change qualitatively the clot evolution, but affects all measurements expressed in time that are related to platelets. The most important values that are affected are the core growth rate (expressed in platelets per second) and the platelet activation time t_c.

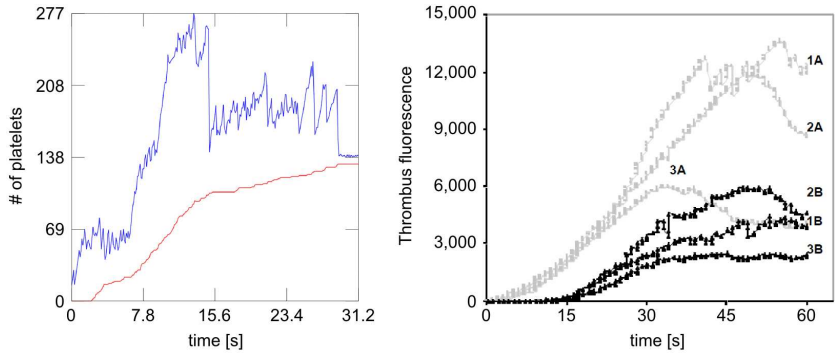

Fig. 5 Left: Platelet clot (blue) and clot core (red) growth in time obtained in simulation. Oscillations in the platelet clot size occur because some part of the clot or individual platelets can be detached by the flow. Right: experimental results for course of incorporation of platelets (A) and fibrin (B) into arterial thrombi for three separate cases (denoted by 1, 2, 3). Reprinted and adapted by permission from Macmillan Publishers Ltd: Nature Medicine (Falati et al., Nature Medicine 8: 11751180, 2002, 2002. www.nature.com).

3.2 PDE parameters

As mentioned previously, the values of parameters of the concentration equations for the basic simulation were chosen following several criteria. Firstly, the diffusion coefficients were set to correspond to the values used in the continuous coagulation pathways model by Krasotkina et al. [42]. Secondly, the model takes into the account only the effect the fibrin polymer concentration has on platelets, while its influence on blood plasma is not modelled. Because of that the model cannot describe correctly the evolution of fibrin net without the platelet aggregate. Therefore, the remaining parameters were set in such a way that thrombin concentration does not propagate counter flow, as the counter flow propagation would result in a formation of fibrin net outside of the platelet clot. Thirdly, the values were adjusted so that the fibrin net generation and the formation of the clot core occur in a time frame which is close to the experimentally observed clot growth times [46]. The values are listed in the Table 1 (see Appendix).

Taking the chosen values as a starting point, a study was carried out to see the influence of each parameter on clot growth and fibrin net formation. Figure 6 and Figure 7 show the final clot core size and the clot core thickness for different values of each of the parameters of the concentration equations.

The clot core thickness is measured at the place where the stenosis is the most severe, and the value is normalized by the vessel diameter. The diffusion coefficient study (Figure 6 a)), where both the thrombin and the fibrinogen coefficient were varied together, shows that the clot core size decreases as the rate of diffusion increases. For a higher diffusion rate more thrombin is taken away by the flow, while the thrombin concentration protected by the platelet aggregate rises more slowly due to loss of the diffused part. As a result the fibrin polymer production is slower, and finally the final core size is lower at the moment when the weakly aggregated part of the clot ruptures leaving only the non-adhesive part. On the other hand, too small diffusion coefficients enable the more rapid generation of thrombin and, eventually, its counter flow propagation, leading to a formation of fibrin net in the flow.

The variation of the thrombin reaction term coefficient k_1^0 (Figure 6 b)) shows that, for the low values, the clot core is unable to develop as the thrombin concentration quickly goes to zero due to the degradation factor s_1. For the two highest values of k_1^0 shown on the graph the core size is similar to the basic case, but the thrombin propagates counter flow, again resulting in the formation of fibrin net outside of the clot.

The graph for fibrin production coefficient k_3^0 (Figure 6 c)) shows that in the case of too low production rate the size of core decreases. This is due to slow fibrin net formation which results in the smaller core size at the moment when the weakly bound part of the clot is detached by the flow. The higher values of k_3^0 result in approximately constant core size since the reaction is rapid enough to consume all the available fibrinogen quickly at places where thrombin level is high.

The study of the influence of the thrombin degradation coefficient s_1 (Figure 7 a)) shows that too high rate of degradation results in a rapid reduction of thrombin concentration to the zero value, thus disabling the core development. On the other hand, the lower values result in a thrombin propagation counter the flow. The rapid thrombin degradation effect is also present in the case of higher T_0 values.

Figure 7 b) shows the effect of the variation of initial fibrinogen concentration, which is also the normal fibrinogen concentration in the undisturbed flow. The graph shows that the core size increases with the increase of value of F_g^0. This is a result of a more rapid core development, which is still slower than the growth of the platelet aggregate. For too low value of F_g^0 the fibrin clot is unable to develop as the whole platelet aggregate breaks off before the fibrin net is able to form. It is notable that in all of the parameter variations the core height graph is similar to the corresponding core size graph. This indicates that the clot core thickness and length ratio remains similar in all cases and it is not strongly affected by the underlying coagulation pathways model.

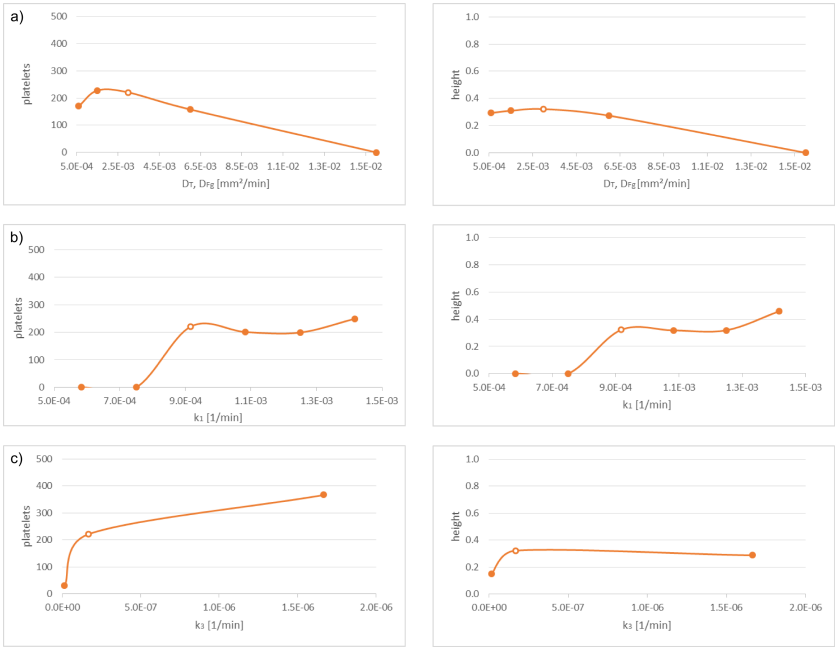

Fig. 6 Variation of values of PDE parameters: a) diffusion coefficients of thrombin D_{T_h} and fibrinogen D_{F_g} (varied together), b) thrombin reaction rate coefficient k_1^0 and c) fibrin polymer reaction rate coefficient k_3^0. Graphs on the left side show final clot size expressed in number of platelets, while the graphs on the right side show the maximal height of the final clot, normalized by the vessel diameter. Empty points denote the result of the single basic simulation with values of parameters given in Table 1 (see Appendix).

3.3 Platelet bond strength

A series of simulations was done to investigate the influence of inter-platelet bond strengths on clot growth. As f_3^A represents a bond between platelets situated in the clot core, covered by fibrin net, it is considered almost unbreakable. Therefore, it was kept at a large constant value of $10nN(= 1 \cdot 10^{-8}N)$ in all simulations. Strength coefficients of the other two types of bonds, f_1^A and f_2^A, were varied in ranges of 0.3 to 0.6, and 0.8 to 1 nN respectively. For each combination of values of f_1^A and f_2^A the activation period t_c was varied in order to find the minimal and the maximal activation time for which clot core successfully develops. Taking into account the experimental studies [47,48] the ratio of a single GPIb bond and a single bond between activated platelets was set to 3 : 8. This ratio can serve as a point of reference, but it is subject to a change because the strength of GPIb bonds depends on the shear rate at the moment of contact [47,48]. Another reason is that the number of bonds established between two platelets is not known. Some attempts were made to establish an estimate of the number of bonds [49,50,51], however they were not experimentally confirmed.

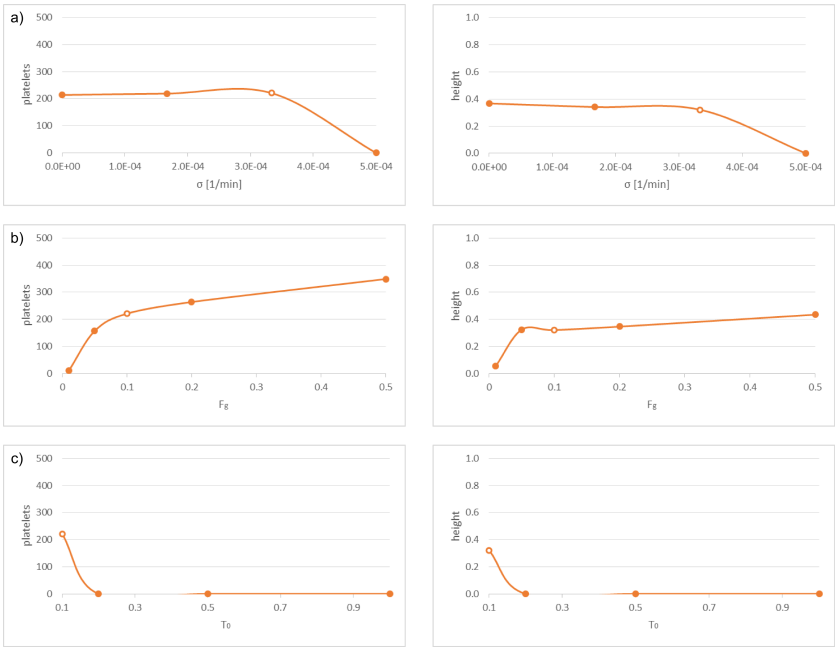

Fig. 7 Variation of values of PDE parameters (continuation): a) thrombin degradation coefficient s_1 , b) initial fibrinogen concentration F_g^0. Graphs on the left side show final clot size expressed in number of platelets, while the graphs on the right side show the maximal height of the final clot, normalized by the vessel diameter. Empty points denote the result of the single basic simulation with values of parameters given in Table 1 (see Appendix).

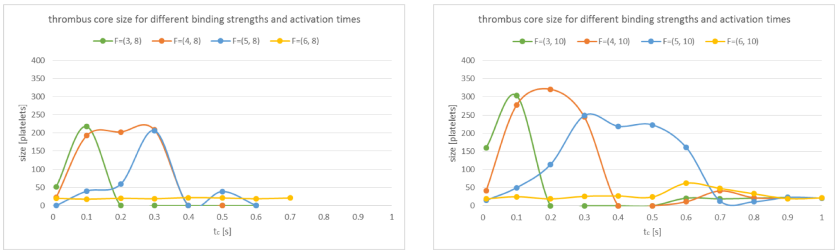

Fig. 8 Variation of strength of platelet forces. The graph on the left side shows clot core sizes for $f_2^A = 0.8$ nN, while the right one shows results for $f_2^A = 1$ nN. In each case f_1^A was varied for values of 0.3, 0.4, 0.5 and 0.6 nN and the activation time was varied between 0.1 and 1 s.

Two graphs in Figure 8 show sizes of the clot core for f_2^A of 0.8 and 1 nN respectively. The four curves on each graph present the results for f_1^A of 0.3, 0.4, 0.5 and 0.6 nN for different activation times t_c. Three types of behaviour were observed for the each combination of values of parameters f_1^A and f_2^A. The first type corresponds to the case when the activation period t_c is too

low. In this case newly aggregated platelets are activated too quickly and the "activated" part of the clot grows too fast. This leads to a breaking of the platelet aggregate before the fibrin net can form and stabilise the clot. The results show that the minimal activation time for which the clot core forms increases significantly as the value of f_1^A increases. Additionally, the higher value of f_2^A decreases the minimal activation time as it allows the "activated" part of the platelet aggregate to grow larger before breaking.

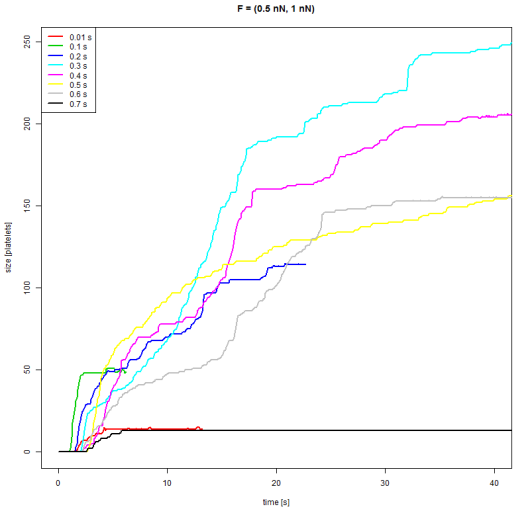

Fig. 9 Clot core growth in first 40 s for values of f_1^A and f_2^A of 0.5 and 1 nN respectively. Each graph corresponds to a different value of activation time t_c - from 0.01 to 0.7 seconds.

The second type of behaviour corresponds to the case where the activation time is in the range of values for which the clot core is able to normally develop. The results show that the higher value of f_2^A allows a higher core size maximum for the same f_1^A value. However, maxima for different values of f_2^A are not achieved for the same activation times.

The third type of behaviour occurs when the activation time is too long, which again results is the inability of clot core to develop. As the activation time is too long, the weakly bound platelet aggregates grow too quickly and break off before any consisting platelets can activate. Hence no activation occurs, and clot cannot sustain the increased shear rate.

Figure 9 shows the growth of the clot core in first 40 seconds for $f_1^A = 0.4$ nN, $f_2^A = 1$ nN, and activation times from 0.01 to 0.7 seconds. For values of the activation time 0.01s and 0.7s the clot was unable to develop. In the case of a too rapid activation the adhering platelets get activated almost immediately after the adhesion, hence the platelet aggregate rapidly grows and breaks off while the clot core is still too small. In the case of the long activation time,

aggregated platelets cannot sustain the increase of the flow shear rate at the surface of the growing clot - they are taken by the flow before they can get activated. Generally speaking, a shorter activation time will have for an effect a faster growth of the platelet aggregate. The growth rate of the fibrin net is bounded by the growth rate of the platelet aggregate, but also by the values of parameters of the system (33). Thus, if the growth of the platelet aggregate is too rapid, the growth rate of the fibrin net becomes bounded by the underlying regulatory network, and the weaker parts of the clot break-off sooner, leaving an undeveloped clot core. This effect is visible in Figure 9 for activation times of 0.1 and 0.2 seconds, while t_c of 0.01 represents a critical case. At the activation time of 0.3 seconds the clot core reaches its maximal value. At longer activation times the clot core growth rate follows more closely the growth rate of the platelet aggregate. As teh fibrin net has also the role of reinforcing the inter-platelet bonds, and thus of supporting the clot growth, the clot and core are able to grow to a larger size. However, if the activation time is longer the weakly bound aggregates at the surface need more time to activate and are thus less prone to the increase of the flow shear rate in the narrowing vessel. Hence, the core growth rate decreases as the activation time increases from the value of 0.3 seconds, where the maximum is achieved.

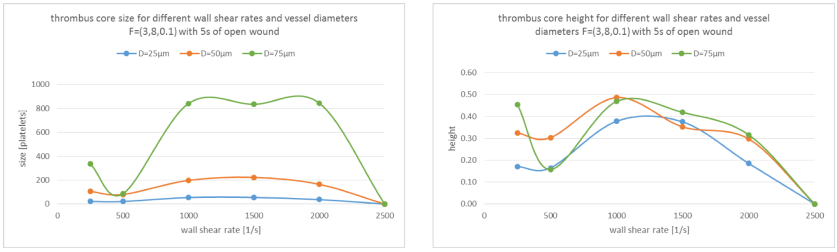

Fig. 10 Variation of flow shear rate (i.e. flow mean velocity) from 250 to 2500 s^{-1} for vessel diameters of 25 (blue), 50 (red), and 75 μm (green). The graph on the left shows the final clot size expressed in number of platelets, while the graph on the right shows the maximal height of the final clot, normalized by the vessel diameter.

3.4 Flow velocity influence

The behaviour of the model was tested in flows of different speeds and in three vessels of different diameters - 25, 50 and 75 μm. In order to have comparable conditions in the near wall region, for all three vessels diameters the flow velocity were varied to correspond to wall shear rates of 250, 500, 1000, 1500, 2000 and 2500 s^{-1}. Furthermore, to avoid that in faster flows the initial level of thrombin concentration at the injury site is immediately taken away by the flow, the level of thrombin at the injury site was kept at value of 1 for the first 5 seconds of the simulation. Figure 10 shows the clot core size and the clot core thickness for each vessel diameter and each wall shear rate.

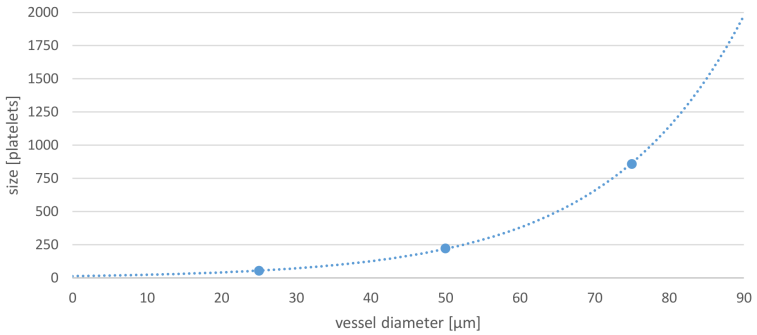

Fig. 11 Final clot size at wall shear rate of 1500 s^{-1} for different vessel diameters. The figure presents an exponential fit with the function $y = 14.046e^{0.055D}$, where y is the final clot size, expressed in the number of platelets, and D is the vessel diameter in micrometres.

The graph of clot core sizes shows that a larger vessel at the same wall shear rate enables development of a larger core. For wall shear rates of 1000, 1500 and 2000 s^{-1} clot and its core were able to fully develop and grow to a larger size. For the chosen values of parameters the shear rate of 2500 s^{-1} was too high for clot to form - platelet aggregates would break-off too soon and the concentration of thrombin was completely washed away. At the wall shear rate of 500 s^{-1} the clot core was able to develop, however its size was smaller in all three vessels. Finally, for the wall shear rate of 250 s^{-1}, the low flow velocity has allowed the counter flow propagation of thrombin, and thus the formation of a fibrin net in the bulk flow, outside of the clot. As mentioned before the model does not describe well the clot formation in the case of counter flow thrombin propagation. Figure 11 shows the relation of the final clot core size and the vessel diameter at the wall shear rate of 1500 s^{-1}, with the exponential function fit.

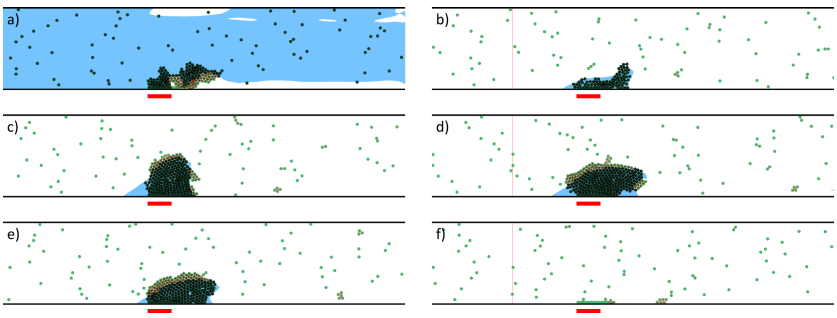

Fig. 12 Final stages of clot growth in the vessel of 50 μm in diameter for different wall shear rates: a) 250 s^{-1}, b) 500 s^{-1}, c) 1000 s^{-1}, d) 1500 s^{-1}, e) 2000 s^{-1} and f) 2500 s^{-1}.

The results for the thickness of the core (Figure 10 right) show that in cases when clot was able to develop, i.e. at wall shear rates of 1000, 1500 and 2000 s^{-1}, the core height has decreased as the flow speed has increased. At the same time the sizes of clot core at the same wall shear rates remained approximately the same for each vessel diameter. This shows that the clot core becomes narrower and more elongated as the flow velocity increases. This behaviour is demonstrated in Figure 12 showing the final clot stages for different wall shear rates in a vessel of 50 μm in diameter. Furthermore, in Figure 10 right, we can see that the ratio of clot core height and diameter of the vessel remains similar for different vessel diameters at the same wall shear rate. This is also demonstrated in Figure 13 where final clot stages are shown for the different vessel diameters at the wall shear rate of 1500 s^{-1}.

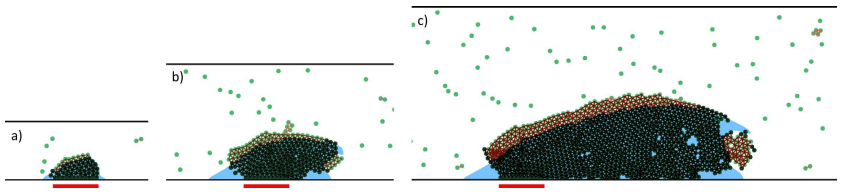

Fig. 13 Final stages of clot growth for wall shear rate of 1500 s^{-1} in a vessel of: a) 25, b) 50 and c) 75μm in diameter.

4 Discussion

The model presented in this paper is based on the biological assumptions which have been experimentally observed. The first premise is that platelet aggregation may precede platelet activation [24,26,27,28,29,30,31]. The second premise is that net of fibrin polymers which forms inside of the clot reinforces the clot structure but also has anti-adhesive properties, which disable further aggregation of platelets [4]. The model based on these assumptions was used to investigate how blood clot stops growing in flow. This is one of the most important problems in the field of haemostasis and thrombosis. Various mechanisms have been previously suggested to act under different conditions, including thrombomodulin-dependent pathway [52], action of flow [53], or fibrin "cap" formation [54]. However, all these mechanisms require fibrin formation, and it is known to be strongly inhibited by the flow [55]. The hereby described model supports the hypothesis that clot stops growing when flow tears of its softer outer part, and leaves only the non-adhesive clot core covered by the fibrin net.

The model shows the following clot growth process. At first an early platelet aggregate forms at the injury site, which is necessary to protect the concentrations of blood factors (especially thrombin) not to be taken by the flow. In that way blood coagulation can occur inside of the platelet clot. As a final product of blood coagulation, fibrin polymer is produced, reinforcing the in-

ner part of the clot, thus forming the clot core. The clot core, which is more stable, can support further clot growth. As the clot grows, the blood vessel becomes narrower and the flow shear rate increases at the top of the clot. Due to the increased shear stress the softer outer parts of the clot, which are not covered by fibrin polymer, are one by one detached and taken by the flow. This process continues until clot stops growing. Two scenarios can occur: a) only non-adhesive clot core remains, unable to adhere new platelets, and b) clot core is covered by a thin layer of activated platelets which can attach new platelets, but the newly aggregated platelets are taken by the flow, due to the increased flow shear rate, before they can be activated.

The model developed in this work is based on the hybrid model described in a previous work [21]. There we have introduced a DPD-PDE method on a model example, containing a single concentration description (fibrin) described by an advection-reaction-diffusion equation. In this work we consider a biologically more realistic DPD-PDE model of blood coagulation and use it to study the mechanism of clot growth. We have introduced a system of partial differential equations, which serves as the minimal model of blood coagulation pathways. The PDE system takes into account the initial activation of prothrombin to thrombin due to presence of tissue factor at the injury site, and the self-accelerated thrombin production (which occurs inside of the clot). Furthermore it models the concentration of fibrinogen which is normally present in blood. Fibrinogen is transformed to fibrin polymer in presence of thrombin, which acts as an enzyme in the reaction. While other blood factors can diffuse in flow, the fibrin polymer concentration is considered to be solid, and thus does not diffuse.

Although this model shows a possible mechanism of clot growth arrest, it is important to note that the hypothesis is tested only for vessels with faster flows (like arterioles and venules), and not for capillaries. Furthermore, in this work we consider two parts of haemostasis, platelet and fibrin clot, and study their interaction. Platelet clot consists of the platelet aggregate, while fibrin clot is a result of biochemical reactions which occur in blood plasma. Together they form a haemostatic plug (blood clot, or simply clot). The model shows how the growth of a platelet clot, supported by a fibrin clot, is limited by flow and the anti-adhesive effect of the fibrin net. However, the model does not take into account the chemical processes which in normal conditions stop the further formation of the fibrin clot, like fibrinolysis and the activation of protein C. These are some of the topics that we plan to pursue in the future works.

Blood cells. At this stage the described model does not take into account other blood cells except platelets. Erythrocytes occupy the bulk flow and push platelets towards the vessel wall. Hence the concentration of platelets is increased in the near wall region. In [44, 45] we have studied cell distribution in flow with a 3D model based on DPD. In future we intend to bring together the coagulation and the 3D cell model and to study the influence of erythrocytes on the clot formation in flow.

Inter-clot flow. One of the important questions is how the intra-clot flow influences the clot growth. In the current 2D model the intra-clot flow is strongly reduced as the aggregated platelets (circles in 2D) form a closed spatial area. However, due to the finite conservative force in DPD the interaction between plasma and platelet particles allows plasma particles to pass through the platelet aggregate. The flow speed inside of the clot is still strongly reduced as clot grows larger. In order to investigate more precisely the effects of the intra-clot flow on the biochemical reactions inside of the clot it is necessary to implement the model in 3D as, in that case, the aggregated platelets (spheres in 3D) will form a porous-like medium.

Dissipative Particle Dynamics. DPD is not a deterministic method due to the random force (equation (3)). Hence each simulation may give different results. However, the extent of the variations of results for simulations with the same values of parameters is limited. It depends on the coefficient of the random force σ compared to strengths of coefficients of other two DPD forces, especially the coefficient of dissipative force γ. The basic simulation (Table 1) and some of the limiting case simulations were repeated several times in order to verify that significant changes in the model behaviour is not coincidental.

Computing performance. DPD as a particle method is quite computationally demanding. Hence we have developed a highly optimised implementation of the described model and adjusted the algorithm for asynchronous parallel computing. With such implementation a single simulation of 30 second clot growth with the values of parameters presented in Table 1 takes about 8 hours to compute on a high-end general purpose PC. Although the model is computationally limited to smaller domains (vessel sizes), larger domains can be efficiently simulated on systems with higher number of processors.

Acknowledgements

The study was supported by the Russian Foundation for Basic Research grants 12-04-00652, 12-04-00438, 14-04-00670 and by the Russian Academy of Sciences Presidium Basic Research Programs “Molecular and Cellular Biology”, “Basic Science for Medicine”, “Integrative Physiology”, “Molecular Mechanisms of Physiologic Functions” and “Russian Federation Presidential Scholarship for Young Scientists and Graduate Students”. The work was also supported by the research grant ANR “Bimod”.

References

1. CDC, Centers for Disease Control and Prevention, *State-specific mortality from sudden cardiac death-United States, 1999.*, MMWR Morb Mortal Wkly Rep. 2002; 51(6): 123-126.

2. Jackson SP, Nesbitt WS, Westein E, *Dynamics of platelet thrombus formation*, J Thromb Haemost 2009; 7 Suppl 1: 17-20.
3. Panteleev MA, Ovanesov MV, Kireev DA, Shibeko AM, Sinauridze EI, Ananyeva NM, Butylin AA, Saenko EL, Ataullakhanov FI, *Spatial propagation and localization of blood coagulation are regulated by intrinsic and protein C pathways, respectively*, Biophys J 2006; 90: 1489-1500.
4. Kamocka MM, Mu J, Liu X, Chen N, Zollman A, Sturonas-Brown B, Dunn K, Xu Z, Chen DZ, Alber MS, Rosen ED, *Two-photon intravital imaging of thrombus development*, J Biomed Opt 2010; 15: 016020.
5. Shibeko AM, Lobanova ES, Panteleev MA, Ataullakhanov FI, *Blood flow controls coagulation onset via the positive feedback of factor VII activation by factor Xa*, BMC Syst Biol 2010; 4: 5.
6. Anand M, Rajagopal K, Rajagopal KR, *A model for the formation, growth, and lysis of clots in quiescent plasma. A comparison between the effects of antithrombin III deficiency and protein C deficiency*, J Theor Biol. 2008 Aug 21;253(4):725-38. Epub 2008 Apr 25. PubMed PMID: 18539301.
7. Anand M, Rajagopal K, Rajagopal KR, *A model for the formation and lysis of blood clots. Pathophysiol Haemost Thromb*, 2005; 34(2-3):109-20. PubMed PMID: 16432312.
8. Bodnar T, Sequeria A, *Numerical Simulation of the Coagulation Dynamics of Blood*, Computational and Mathematical Methods in Medicine, Volume 9 (2008), Issue 2, Pages 83-104
9. Guy RD, Fogelson AL, Keener JP, *Fibrin gel formation in a shear flow*, Math Med Biol. 2007 Mar; 24(1) : 111-30
10. Alenitsyn AG, Kondratyev AS, Mikhailova I, Siddique I, *Mathematical Modeling of Thrombus Growth in Microvessels*, Journal of Prime Research in Mathematics Vol. 4(2008), 195-205
11. Tokarev A, Sirakov I, Panasenko G, Volpert V, Shnol E, Butylin A, and Ataullakhanov F, *Continuous Mathematical Model of Platelet Thrombus Formation in Blood Flow*, Russian Journal of Numerical Analysis and Mathematical Modelling. Vol. 27, No. 2, pp.192-212., 2012.
12. Pivkin IV, Richardson PD, Karniadakis G, *Blood flow velocity effects and role of activation delay time on growth and form of platelet thrombi*, PNAS 2006, 103, 17164-17169
13. Pivkin IV, Karniadakis GE, *A new method to impose no-slip boundary conditions in dissipative particle dynamics*, J. Comp. Phys. 207 (2005) 114-128.
14. Xu Z, Chen N, Kamocka MM, Rosen ED, Alber M, *A multiscale model of thrombus development*, J. R. Soc. Interface (2008) 5, 705722
15. Xu Z, Lioi J, Mu J, Kamocka MM, Liu X, Chen DZ, Rosen ED, Alber M, *A Multiscale Model of Venous Thrombus Formation with Surface-Mediated Control of Blood Coagulation Cascade*, Biophysical Journal, vol. 98 (2010) 17231732
16. Xu Z, Chen N, Shadden S, Marsden JE, Kamocka MM, Rosen ED, Alber M, *Study of Blood Flow Impact on Growth of Thrombi Using a Multiscale Model*, Soft Matter, 2009,5, 769-779
17. Xu Z, Christleyy S, Lioiz J, Kim O, Harveyx C, Sun W, Rosen ED, Alber M, *Multiscale Model of Fibrin Accumulation on the Blood Clot Surface and Platelet Dynamics*, Methods in Cell Biology, vol. 110, 2012
18. Sweet CR, Chatterjee S, Xu Z, Bisordi K, Rosen ED, Alber M, *Modelling platelet - blood flow interaction using the subcellular element Langevin method*, J. R. Soc. Interface (2011) 8, 17601771
19. Fogelson AL, *Cell-based Models of Blood Clotting*, Single-Cell-Based Models in Biology and Medicine (ed. by Anderson ARA, Chaplain MAJ, Rejniak KA), Mathematics and Biosciences in Interaction, p. 234-169, Birkhäuser Verlag Basel, 2007.
20. Tosenberger A, Ataullakhanov F, Bessonov N, Panteleev M, Tokarev A, Volpert V, *Modelling of thrombus growth and growth stop in flow by the method of dissipative particle dynamics*, Russian Journal of Numerical Analysis and Mathematical Modelling, 2012, Vol. 27, No. 5, pp. 507-522
21. Tosenberger A, Ataullakhanov F, Bessonov N, Panteleev M, Tokarev A, Volpert V, *Modelling of thrombus growth in flow with a DPD-PDE method*, Journal of Theoretical Biology 337, 2013, pp. 3041

22. Filipovic N, Kojic M, Tsuda A, *Modelling Thrombosis Using Dissipative Particle Dynamics Method*, Phil. Trans. R. Soc. A 2008 366, 3265-3279
23. Pivkin IV, Richardson PD, Karniadakis GE, *Effect of Red Blood Cells on Platelet Aggregation*, Engineering in Medicine and Biology Magazine, IEEE 28.2 (2009): 32-37
24. Jackson SP, *The growing complexity of platelet aggregation*, Blood. 2007 Jun 15; 109(12): 5087-95. Epub 2007 Feb 20.
25. Fogelson AL, Guy RD, *Immersed-Boundary-Motivated Models of Intravascular Platelet Aggregation*, Comput. Methods Appl. Mech. Eng., Vol. 197, 2250-2264 (2008)
26. Kulkarni S, Dopheide SM, Yap CL, Ravanat C, Freund M, Mangin P, Heel KA, Street A, Harper IS, Lanza F, Jackson SP, *A revised model of platelet aggregation*, J Clin Invest. 2000 Mar;105(6):783-91.
27. Jen CJ, Hu SJ, Wu HJ, Lin TS, Mao CW, *Platelet-fibrin interaction in the suspension and under flow conditions*, Adv Exp Med Biol. 1990;281:277-85. PubMed PMID: 2102618.
28. Jen CJ, Lin JS, *Direct observation of platelet adhesion to fibrinogen- and fibrin-coated surfaces*, Am J Physiol. 1991 Nov;261(5 Pt 2):H1457-63. PubMed PMID: 1951733.
29. Jen CJ, Tai YW, *Morphological study of platelet adhesion dynamics under whole blood flow condition*, Platelets 1992;3(3):145-53. PubMed PMID: 21043907.
30. Chiu YL, Chou YL, Jen CY, *Platelet deposition onto fibrin-coated surfaces under flow conditions*, Blood Cells, 1988;13(3):437-50. PubMed PMID: 3382750.
31. Zaidi TN, McIntire LV, Farrell DH, Thiagarajan P, *Adhesion of platelets to surface-bound fibrinogen under flow*, Blood. 1996 Oct 15;88(8):2967-72. PubMed PMID: 8874193.
32. Frojmovic MM, Mooney RF, Wong T, *Dynamics of platelet glycoprotein IIb-IIIa receptor expression and fibrinogen binding. I. Quantal activation of platelet subpopulations varies with adenosine diphosphate concentration* Biophys J. 1994 Nov;67(5):2060-8.
33. Fedosov DA, *Multiscale Modeling of Blood Flow and Soft Matter*, PhD dissertation at Brown University, (2010).
34. Groot RD, Warren PB, *Dissipative particle dynamics: Bridging the Gap Between Atomistic and Mesoscopic Simulation*, J. Chem. Phys., 107 (1997) (11), 4423–4435.
35. Karttunen M, Vattulainen I, Lukkarinen A, *A novel methods in soft matter simulations*, Springer, Berlin, 2004.
36. Allen MP, Tidesley DJ, *Computer Simulation of Liquids*, Clarendon, Oxford, 1987.
37. Fedosov DA, Pivkin IV, Karniadakis GE, *Velocity limit in DPD simulations of wall-bounded flows*, J. Comp. Phys. 227 (2008) 25402559.
38. Schiller UD, *Dissipative Particle Dynamics. A Study of the Methodological Background*, Diploma thesis at Faculty of Physics University of Bielefeld, 2005
39. Weisel JW, *Enigmas of Blood Clot Elasticity*, Science 320, 456 (2008).
40. Brown AEX, Litvinov RI, Discher DE, Purohit PK, Weisel JW, *Multiscale Mechanics of Fibrin Polymer: Gel Stretching with Protein Unfolding and Loss of Water*, Science 325, 741 (2009).
41. Windberger U, Bartholovitsch A, Plasenzotti R, Korak KJ, Heinze G, *Whole blood viscosity, plasma viscosity and erythrocyte aggregation in nine mammalian species: reference values and comparison of data*, Exp. Physiol. 2003, 88:431-440.
42. Krasotkina YV, Sinauridze EI, Ataullakhanov FI, *Spatiotemporal dynamics of fibrin formation and spreading of active thrombin entering non-recalcified plasma by diffusion*, Biochimica et Biophysica Acta 1474, (2000), 337-345
43. Pallister CJ and Watson MS, *Haematology*, Scion Publishing, 2010.
44. Bessonov N, Babushkina E, Golovashchenko FG, Tosenberger A, Ataullakhanov F, Panteleev M, Tokarev A, Volpert V, *Numerical Simulations of Blood Flows With Non-uniform Distribution of Erythrocytes and Platelets*, Russian Journal of Numerical Analysis and Mathematical Modelling, vol. 28 (2013), no. 5, in press
45. Bessonov N, Babushkina E, Golovashchenko FG, Tosenberger A, Ataullakhanov F, Panteleev M, Tokarev A, Volpert V, *Numerical Modelling of Cell Distribution in Blood Flow*, Math. Model. Nat. Phenom., submitted
46. Falati S, Gross P, Merrill-Skoloff G, Furie BC, Furie B, *Real-time in vivo imaging of platelets, tissue factor and fibrin during arterial thrombus formation in the mouse*, Nat Med 2002; 8: 1175-1181.

47. Arya M, Kolomeisky AB, Romo GM, Cruz MA, López JA, Anvari B, *Dynamic Force Spectroscopy of Glycoprotein Ib-IX and von Willebrand Factor*, Biophysical Journal, Vol. 88, June 2005, pp. 43914401
48. Litvinov RI, Bennett JS, Weisel JW, Shumanz H, *Multi-Step Fibrinogen Binding to the Integrin $\alpha IIb\beta 3$ Detected Using Force Spectroscopy*, Biophysical Journal, Vol. 89, October 2005, pp. 28242834
49. Wagner CL, Mascelli MA, Neblock DS, Weisman HF, Coller BS, Jordan RE, *Analysis of GPIIb/IIIa Receptor Number by Quantification of 7E3 Binding to Human Platelets*, Blood. 1996 Aug 1; 88 (3) : 907-14.
50. Coburn LA, *Studies of Platelet GPIb-alpha and von Willebrand Factor Bond Formation Under Flow*, PhD thesis at Georgia Institute of Technology and Emory University, (May 2010).
51. Wellings PJ, *Mechanisms of Platelet Capture Under Very High Shear*, Master thesis at Georgia Institute of Technology, (May 2011).
52. Panteleev MA, Ovanesov MV, Kireev DA, Shibeko AM, Sinauridze EI, Ananyeva NM, Butylin AA, Saenko EL, Ataullakhanov FI, *Spatial propagation and localization of blood coagulation are regulated by intrinsic and protein C pathways, respectively*, Biophys J., 2006 Mar 1, 90(5), 1489-500.
53. Barynin IA, Starkov IA, Khanin MA, *Mathematical models in hemostasis physiology*, Izv Akad Nauk Ser Biol. 1999, (1):59-66 (in Russian).
54. Kamocka MM, Mu J, Liu X, Chen N, Zollman A, Sturonas-Brown B, Dunn K, Xu Z, Chen DZ, Alber MS, Rosen ED, *Two-photon intravital imaging of thrombus development*, J. Biomed. Opt. 2010, 15(1):016020.
55. Shibeko AM, Lobanova ES, Panteleev MA, Ataullakhanov FI, *Blood flow controls coagulation onset via the positive feedback of factor VII activation by factor Xa*, BMC Syst. Biol. 2010, 4:5.
56. Tosenberger A, Salnikov V, Bessonov N, Babushkina E, Volpert V, *Particle Dynamics Methods of Blood Flow Simulations*, Math. Model. Nat. Phenom. 6 (2011), no. 5, 320–332.
57. Panteleev MA, Ovanesov MV, Kireev DA, Shibeko AM, Sinauridze EI, Ananyeva NM, Butylin AA, Saenko EL, Ataullakhanov FI, *Spatial propagation and localization of blood coagulation are regulated by intrinsic and protein C pathways, respectively*, Biophys J. 2006 Mar 1; 90(5) : 1489-500.
58. Dashkevich NM, Ovanesov MV, Balandina AN, Karamzin SS, Shestakov PI, Soshitova NP, Tokarev AA, Panteleev MA, Ataullakhanov FI, *Thrombin activity propagates in space during blood coagulation as an excitation wave*, Biophys J. 2012 Nov 21; 103(10) : 2233-40
59. Wooton DM, Ku DN, *Fluid mechanics of vascular systems and thrombus*, Annu. Rev. Biomed. Eng. 1999. 01 : 299329

5 Appendix

5.1 Boundary conditions for DPD

As with other particle methods, an important and delicate question is how to define boundary conditions. To simulate a part of blood vessel in our 2D model, three types of boundaries are used - solid, inflow and outflow. Depending on the choice of solid boundary conditions, problems like density oscillations and errors in the velocity profile can occur [37,56,13]. Figure 14 shows correct density and velocity profiles for Poiseuille flow obtained with the use of the solid boundary conditions described below.

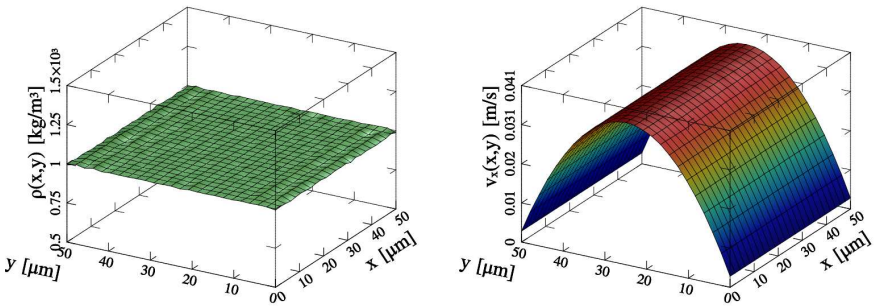

Fig. 14 Density and velocity profiles in Poiseuille flow obtained by DPD with the described no-slip boundary conditions. Reprinted by permission from Journal of Theoretical Biology (Tosenberger et al. 2012 [21]).

The no-slip solid boundary model, which represents the blood vessel wall, is modelled in the following way: if a particle p is on a distance $r < r_c$ from the solid boundary, there exists an mirror image p' of the particle p on the other side of the boundary with the velocity opposite to velocity of particle p ($\mathbf{v}_{p'} \equiv -\mathbf{v}_p$). This can seem like adding a fair number of new particles, which can decrease the simulation performance. However, combined with the above described method for the separation of the simulation area on boxes, it can be efficiently implemented without any real addition of new particles. All the mirrored particles are mirror images of particles which are in the boxes connected to the solid boundaries. Therefore, when we calculate forces between two particles in the simulation domain, p_1 and p_2, if they are positioned in the boxes which are connected to the same solid boundary, we can calculate the force of the imaginary particle p_1' on the particle p_2 and p_2' on p_1. Additionally, if particle p is on $r < \frac{1}{2}r_c$ distance from the boundary, the force from p' on p is calculated. The described boundary conditions act as no-slip boundary for DPD, and ensure that both, density and velocity, profiles are correct.

In the simulation of clot growth in flow the numbers of platelets which enter the domain at inflow boundary and those which exit the domain at outflow boundary are not equal as some platelets will become part of the clot and be contained in the domain. Hence, the constant inflow of platelets cannot be simulated by periodic boundary conditions, and more complex methods have to be used. One approach is to define a particle generation area (GA) at the inflow part of the domain, as shown in Figure 15. The generation area (GA) works independently of the remaining part of the simulation domain - simulation area (SA). The solid boundaries in GA are modelled in the same way as in SA, but the inflow and outflow boundaries are modelled as periodic boundaries, meaning that the particle that exits GA on the outflow boundary reappears on the GA inflow boundary, creating an infinite flow loop. Also particles from SA do not influence the particles from GA, but the particles from GA can influence the particles from SA. For each particle which crosses the GA outflow boundary an exactly same copy is made at the SA inflow boundary, and that new particle is being joined to SA. Once the particle has been joined to SA, it can return for a short time in GA, but it remains assigned to SA and does not influence particles from GA. Furthermore, when it crosses back from GA to SA, it does not generate a new particle. All this insures the integrity and correctness of GA and also the non-biased creation of particles for SA.

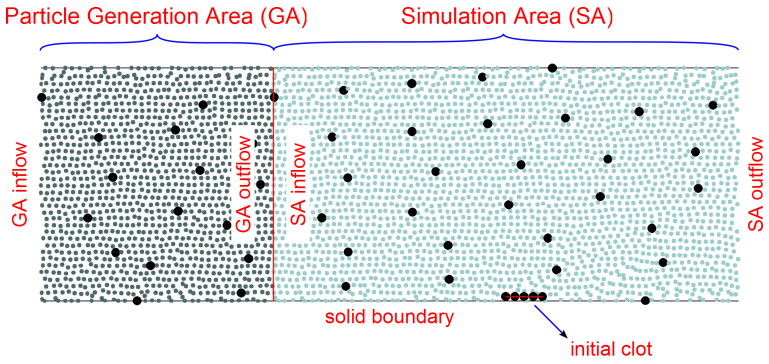

Fig. 15 Particle Generation Area (GA) and Simulation Area (SA). Reprinted by permission from Journal of Theoretical Biology (Tosenberger et al. 2012 [21]).

On the SA outflow boundary particles which exit the simulation domain are being deleted. In order to keep the balance of DPD forces near the outflow boundary, one way periodic boundary conditions are used. The GA inflow and SA outflow boundaries are paired, as it is normally done when using the periodic boundary conditions. However, only the particles form the inflow boundary layer can influence the particles in the outflow boundary layer, while in the opposite direction particles do not influence each other. This way, at the outflow boundary a correct velocity and density profiles are enforced, while

the generation area remains a closed system. Figure 15 shows a scheme of the simulation and generation areas. The method is similar to a method used in [23].

5.2 Values of parameters for the basic simulation

DOMAIN	Value	Physical	Description
L	200	200 μm	length of the simulated blood vessel
L_{GA}	50	50 μm	length of the Particle Generation Area (GA)
D	50	50 μm	diameter of the simulated blood vessel
G_x	7200	72 m/s^2	external force in x direction used to induce flow
$\bar{v}_x$	187.5	18.75 mm/s	average flow velocity
w_x		1500 s^{-1}	wall shear rate
DPD	Value	Physical	Description
a_{ij}	600000		conservative force coefficient
γ	3550		dissipative force coefficient
σ	20000		random force coefficient
r_c	5		force cut-off radius
k	1		exponent in the equation (6)
k_BT	1		the Boltzmann constant times temperature
n	0.36		particle number density
m	0.463		particle mass
dt_{DPD}	0.001		DPD time step
PDE	Value	Physical	Description
dx	0.5	0.5 μm	spatial step
dt_{PDE}	0.01	0.1 ms	PDE time step
D_{T_h}	0.5	0.003 mm/min	thrombin diffusion coefficient
k_1^0	5.5	$3.3 \cdot 10^4$ min^{-1}	thrombin reaction term coefficient
T_0	0.1		thrombin reaction term coefficient
C_0	1		thrombin reaction term coefficient
s_1	2	$1.2 \cdot 10^4$ min^{-1}	thrombin degradation coefficient
D_{F_g}	0.5	0.003 mm/min	fibrinogen diffusion coefficient
k_3^0	0.001	6 min^{-1}	fibrinogen reaction term coefficient
c_{F_p}	0.8		critical fibrin polymer level
OTHER	Value	Physical	Description
f_1^A	$3 \cdot 10^6$	0.3 nN	weak inter-platelet bond coefficient
f_2^A	$8 \cdot 10^6$	0.8 nN	activated inter-platelet bond coefficient
f_3^A	$1 \cdot 10^8$	10 nN	fibrin net reinforced bond coefficient
t_c	10	0.1 s	platelet activation period
τ	10	0.1 s	DPD-PDE data exchange period
p	0.017	$3.672 \cdot 10^12$ L^{-1}	platelet frequency

Table 1 Values of all parameters in the basic simulation.